GPPS Chania22, September 11, 2022
CFD Workshop

DV7-1487

Validation of improved SA model on Various Cascades Part1 : Numerical Simulation Result on BUAA cascade

IHI

2022/9/11

IHI Corporation
Core Technology & System Engineering Gr.
Advanced Technology Department
Research & Engineering Division
Naoki Tani

For CFD workshop

- Validation and verification of RANS analysis

  Comparison of other CFD code at the same RANS model can reveal each solver characteristics.

For CFD technology development

- Validation of improved RANS

  - ➢ There are several researches on improved RANS model, however, validation cases with these improved models are limited.
    - ➢ This CFD workshop is good chance to validate improved model.
  - ➢ Impact of unsteady CFD was also validated.

BUAA cascade is appropriate for low Mach number validation.

CFD code : UPACS

IHI

- UPACS (Originally developed by JAXA)
- Cell centered
- Multi block structured grid

Kazawa, Junichi, et al. "Numerical study on fan noise generated by rotor-stator interaction." 13th AIAA/CEAS Aeroacoustics Conference (28th AIAA Aeroacoustics Conference). 2007.

- MUSCL interpolated 3rd order scheme
- Matrix free Gauss-Sidel time integration
  - 2nd order accuracy in time with newton sub-iteration
- Buffer-layer type non-reflective mixing plane
- Spallart-Allmaras turbulence model
  - SA and optimized SA-R-H-QCR2000(Steady and Unsteady)
- Density base solver
  - Low Mach-number preconditioning is applied for better convergence.

Blue character part is different from TUDA cases.

Kitamura, Keiichi, et al. "Performance of low-dissipation euler fluxes and preconditioned implicit schemes in low speeds." *48th AIAA Aerospace Sciences Meeting Including the New Horizons Forum and Aerospace Exposition*. 2010.

Colin, Y., H. Deniau, and J-F. Boussuge. "A robust low speed preconditioning formulation for viscous flow computations." *Computers & Fluids* 47.1 (2011): 1-15.

Classical mixing plane

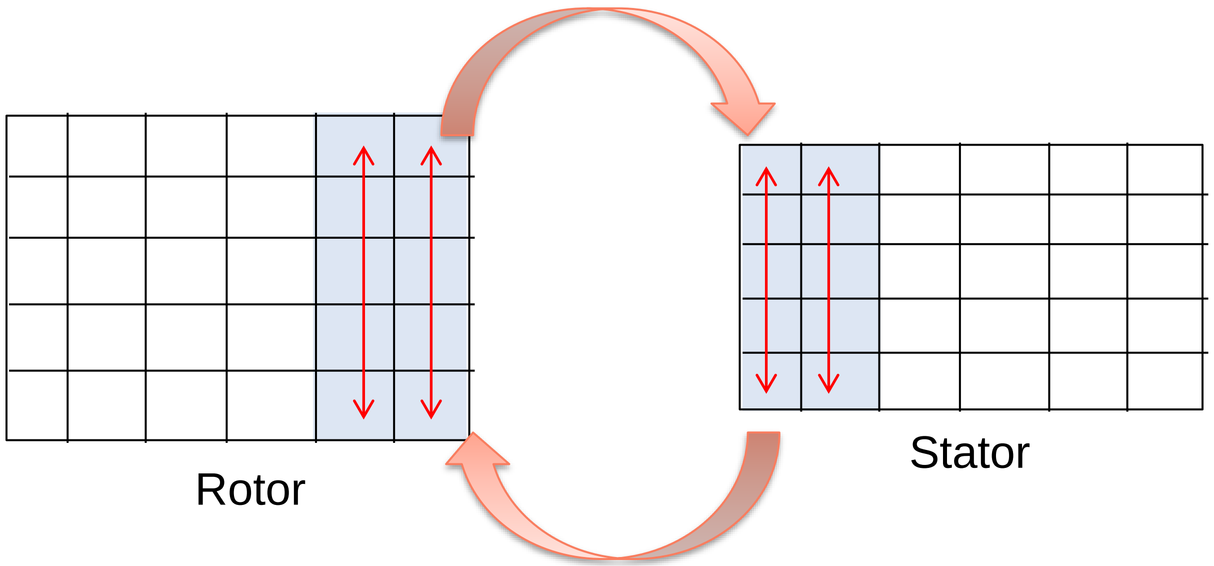

1. Circumferential averaging
2. Exchange data between R/S
3. NRBC operation (option)

Buffer-layer type non-reflective mixing plane

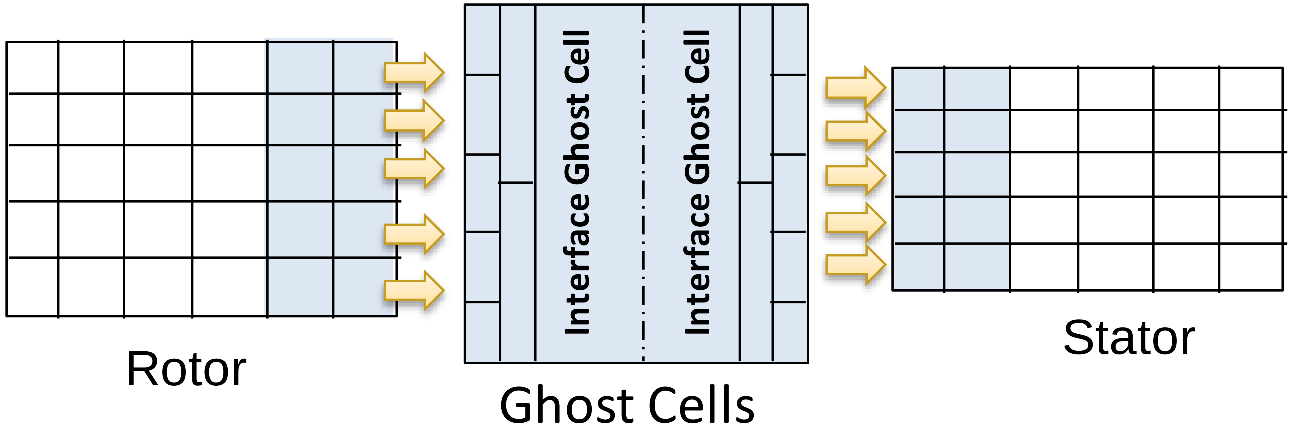

1. Generate ghost cells between R/S.
2. Coarsening to 1 cell at the interface.
3. Both inner and ghost cells are solved simultaneously

Turbulence model: SA-R-H-QCR2000

IHI

Matsui K., et al. “CALIBRATED ROTATION-HELICITY-QUADRATIC CONSTITUTIVE RELATION SPALARTALLMARAS (R-H-QCR SA) MODEL FOR THE PREDICTION OF MULTI-STAGE COMPRESSOR CHARACTERISTICS.” *Proceedings of ASME Turbo Expo 2022Turbomachinery Technical Conference and Exposition, GT2022-82080*

SA-R-H-QCR2000

SA-R: Rotation correction.

Reduce turbulence generation at rigid rotation part.

$$S_{SA-R} = S_{SA} + C_{rot} min(0, S - \Omega)$$

SA-H: Helicity modification.

Consideration of turbulence backscatter.

$$f_h = 1 + c_{h1}\widehat{H}^{c_{h2}}$$

$$\widehat{H} = \frac{\boldsymbol{u} \cdot \boldsymbol{\Omega}}{|u||\Omega|}$$

SA-QCR2000: Quadratic Constitutive Relation.

SA model which can consider anisotropic effect.

$$\tau_{ij_{QCR}} = \tau_{ij} - C_{cr1}[O_{ik}\tau_{jk} + O_{jk}\tau_{ik}], \qquad C_{cr1} = 0.3$$

$$O_{ij} = 2W_{ij} \Big/ \sqrt{\frac{\partial u_m}{\partial x_n}\frac{\partial u_m}{\partial x_n}}, W_{ij} = \frac{1}{2}\left(\frac{\partial u_i}{\partial x_j} - \frac{\partial u_j}{\partial x_i}\right)$$

Model constants are optimized with Polynomial Chaos Method.

Computational grid and boundary conditions

IHI

Official grid was not used.

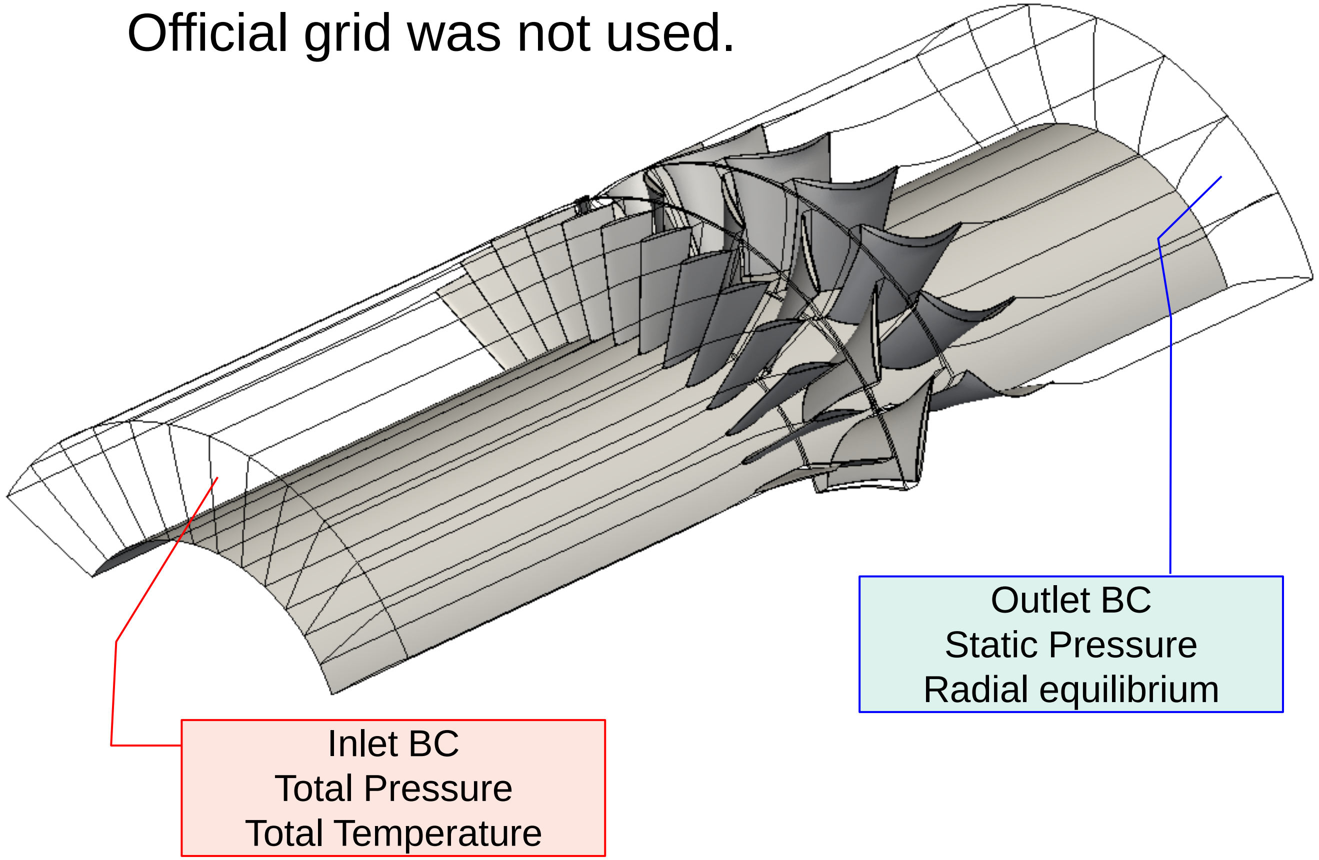

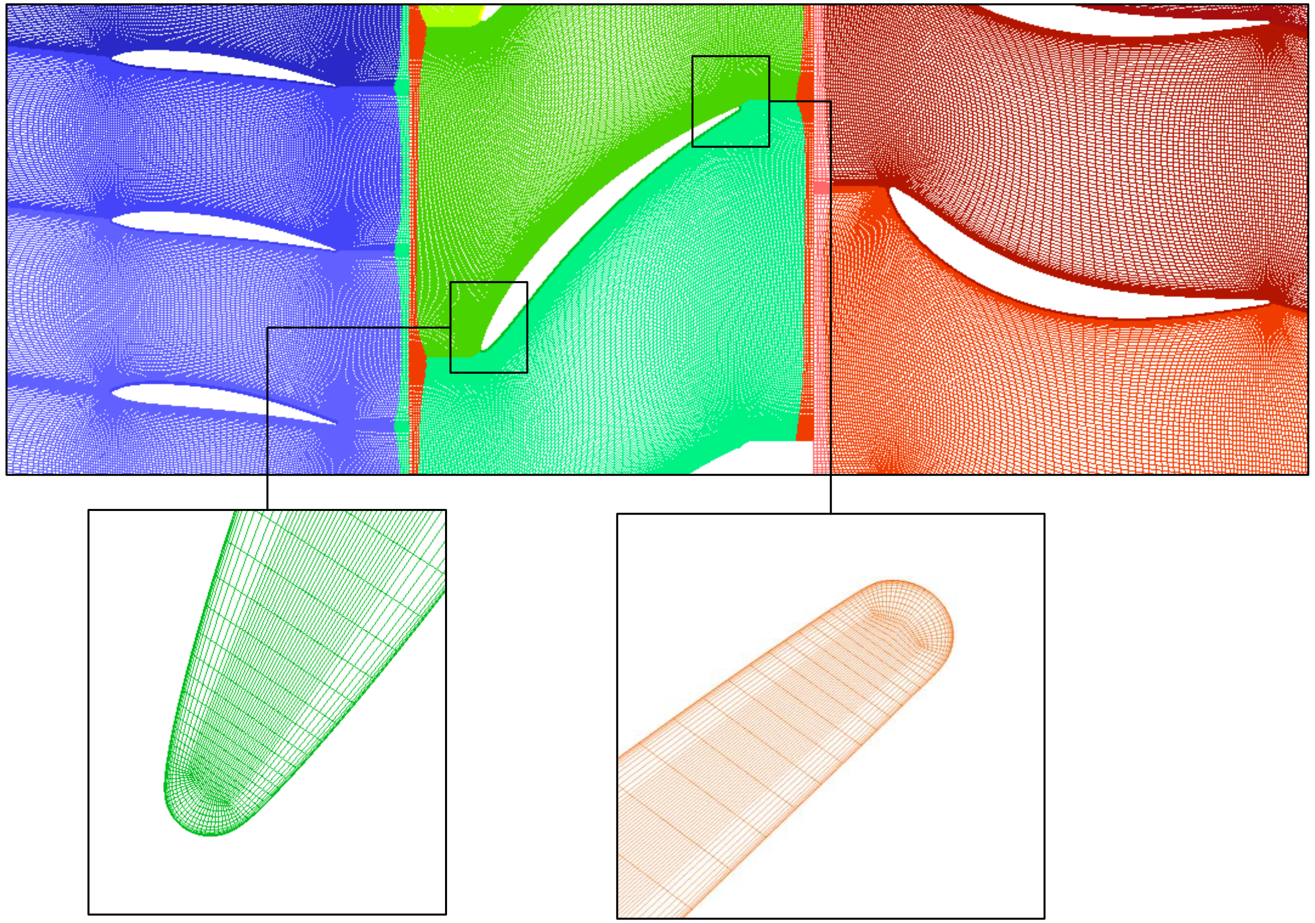

Inter-blade and tip-clearance grid topology

- Grid Topology : O-H
  - Max centroid skewness is 0.71
  - Y+~3 with 1.2 growth rate
- Total grid point : 1.8M(Steady) and 53M(Unsteady 1/4round)
- Computational resources
  - Steady : 20 cores 9 hours per case
  - Unsteady : 40 cores 30 hours 4 rotation per case

Computational results 1
Steady Analysis: SA vs. SA-R-H-QCR2000

Turbulence model

- Static pressure rise coefficient shows slightly higher than that of experiment.
- Optimized R-H-QCR show smaller stall mass flow coefficient than that of pure SA model.
- SA shows slightly higher stall mass flow coefficient, but R-H-QCR show smaller than the experimental result.

In stall condition. Flow rate is decreasing. CFD runs are not converged.

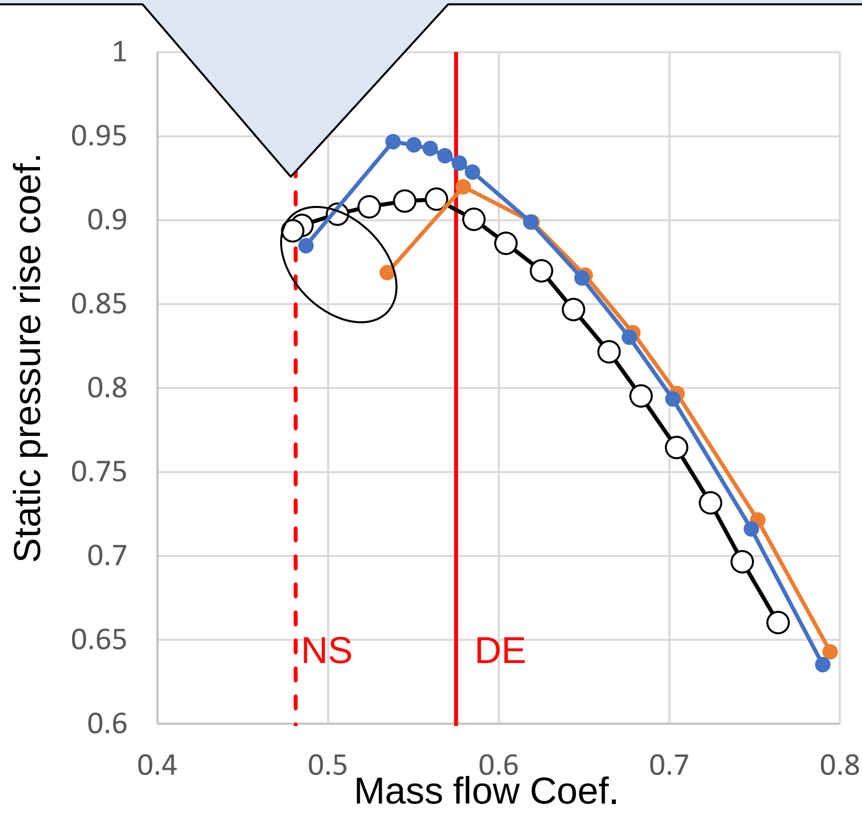

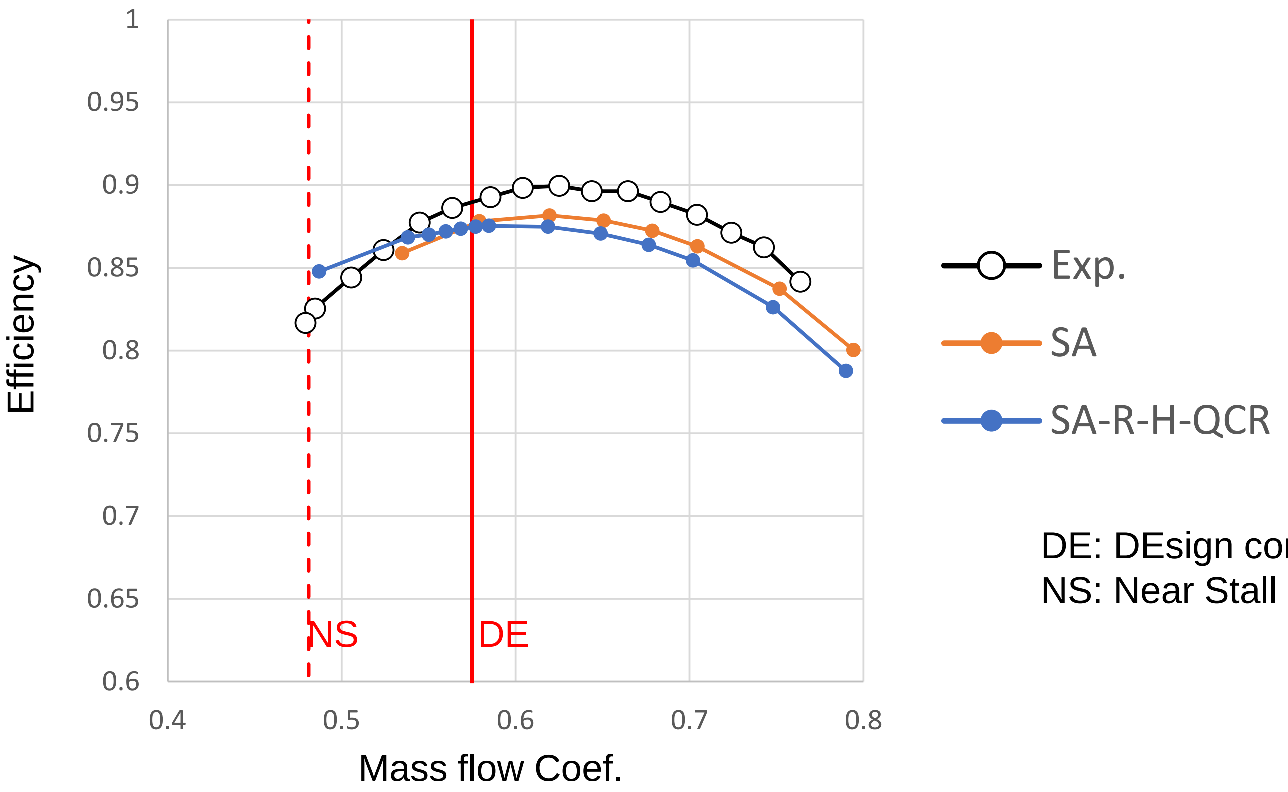

DE: DEsign condition
NS: Near Stall condition

Stator suction surface oilflow comparison at NS condition

Blue: Backflow Region

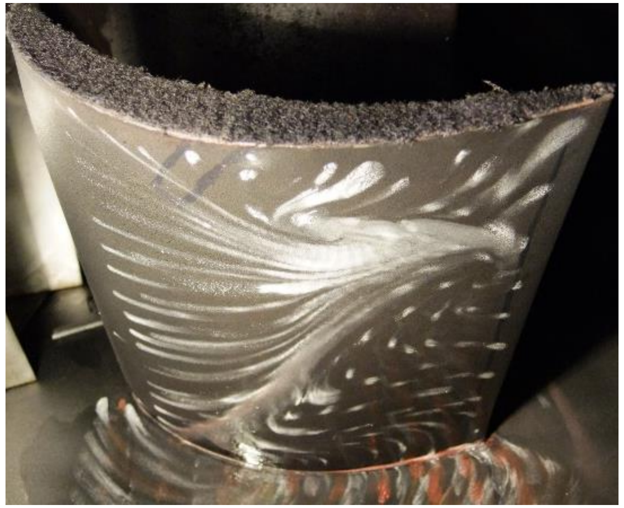

Exp.

SA

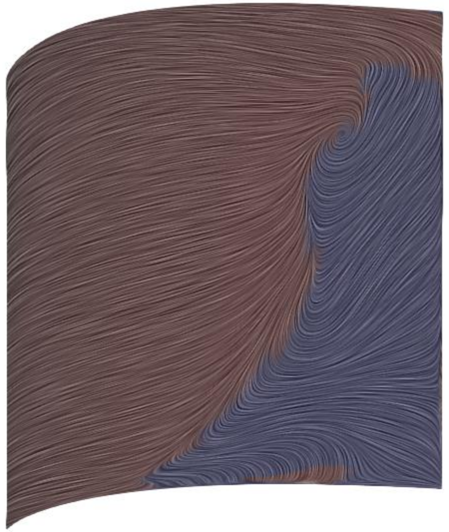

SA-R-H-QCR

- In experiment, both hub and shroud separation can be observed.
  - Hub separation cannot be reproduced with SA. Casing side separation is also too small.
  - SA-R-H-QCR can reproduce massive corner separation, but casing separation cannot be seen.

Computational results 2
Unsteady CFD

Note : Blade numbers are modified from 36-17-20 to 36-18-21 (1/3 circumference).
Calculation is restarted from steady calculation.

SA-R-H-QCR model result

IHI

- Unsteady R-H-QCR model shows better agreement at high flow rate condition.
- However, stall mass flow coefficient becomes higher in unsteady case.
- Efficiency is still smaller than experiment. Highest efficiency flow coefficient agrees well in unsteady case.

Question : Which phenomena derives this difference?

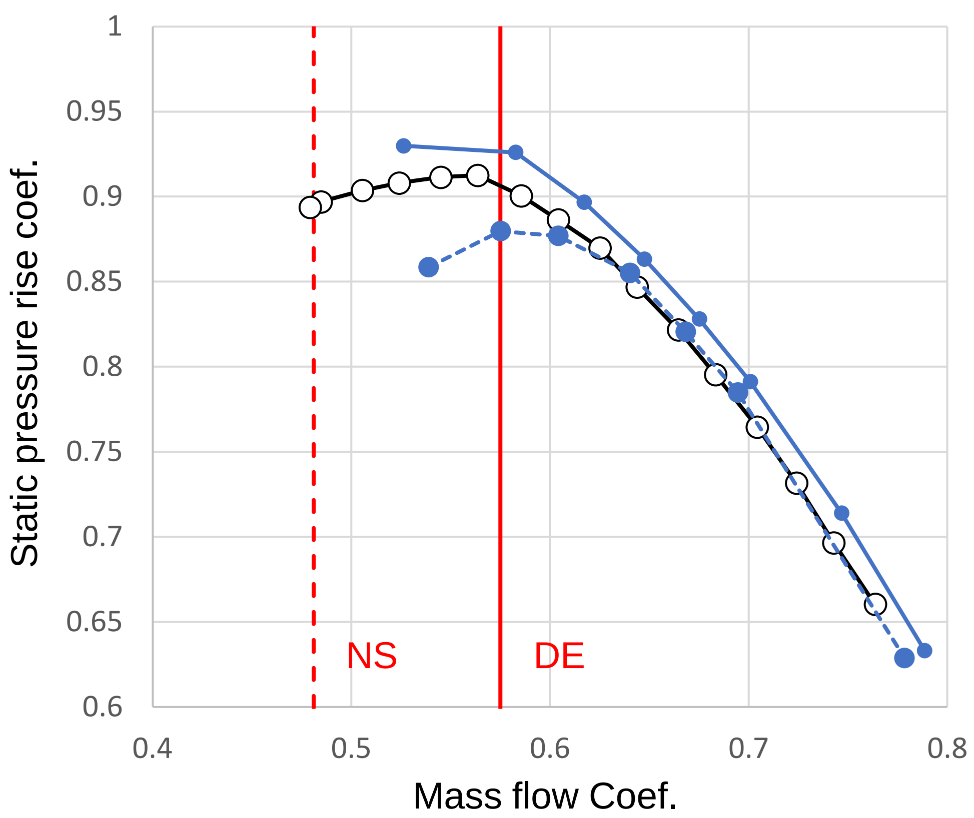

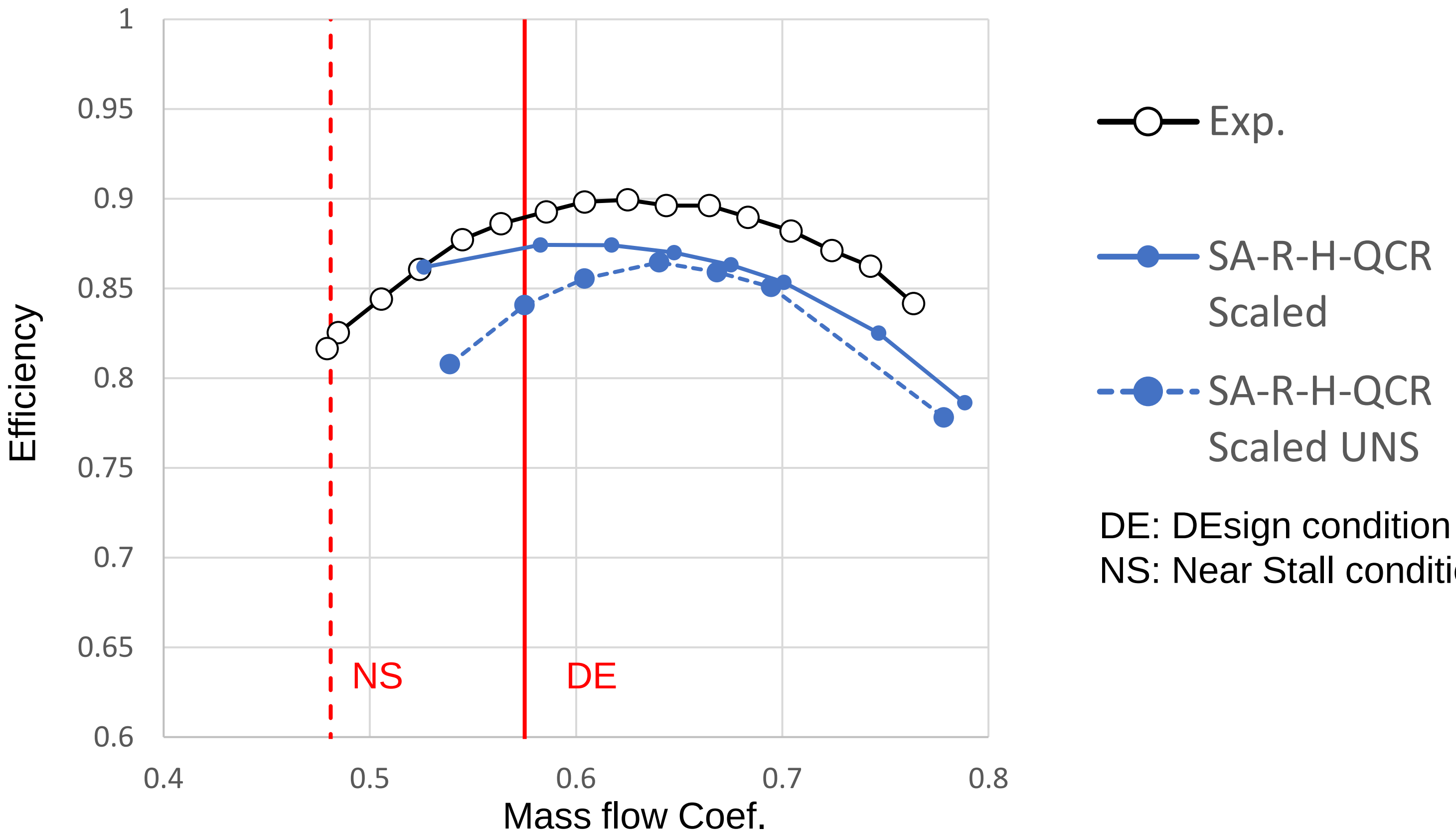

DE: DEsign condition
NS: Near Stall condition

Stator suction surface oilflow comparison : SA-R-H(BS)-QCR

IHI

- Major difference is caused by stator flow.
    - Separation pattern at DE condition is different.
    - Backflow region near tip cannot be seen in unsteady cases.
    - Flow pattern is different between blade to blade in DE unsteady case.

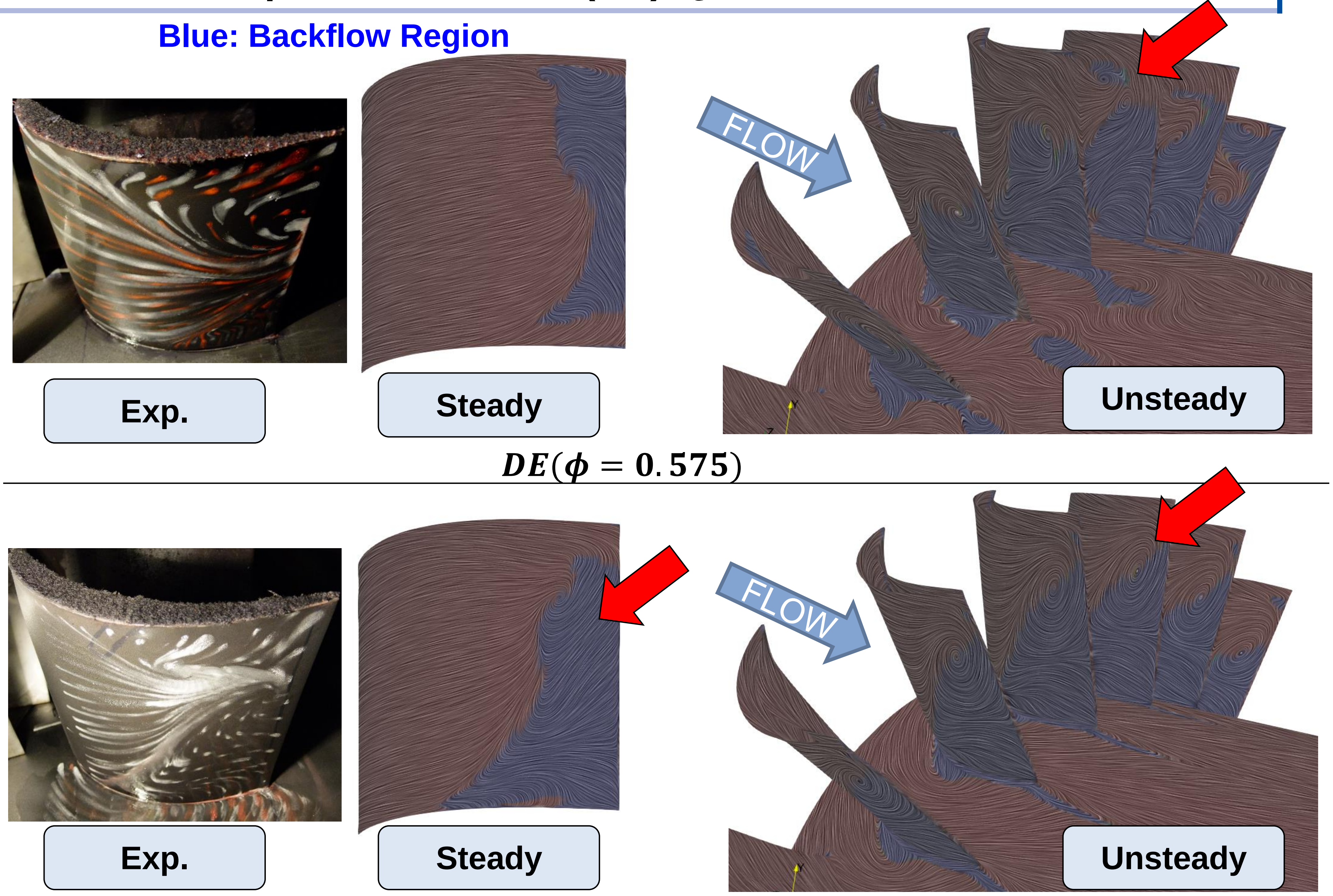

$NS(\phi = 0.481)$

Impact of mixing plane

- Flow angle at rotor outlet (dashed line) is almost identical.
- Stator inlet flow angle is slightly decreased for steady analysis caused by mixing plane.
  - Flow angle difference is approximately 0.7 degree near hub.

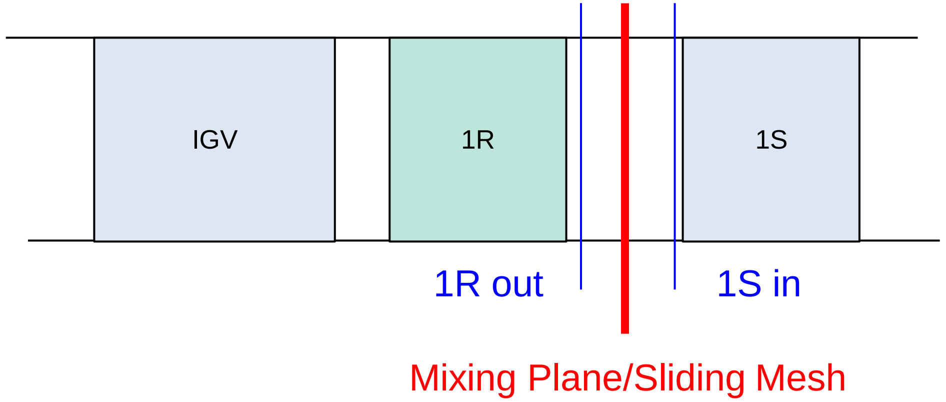

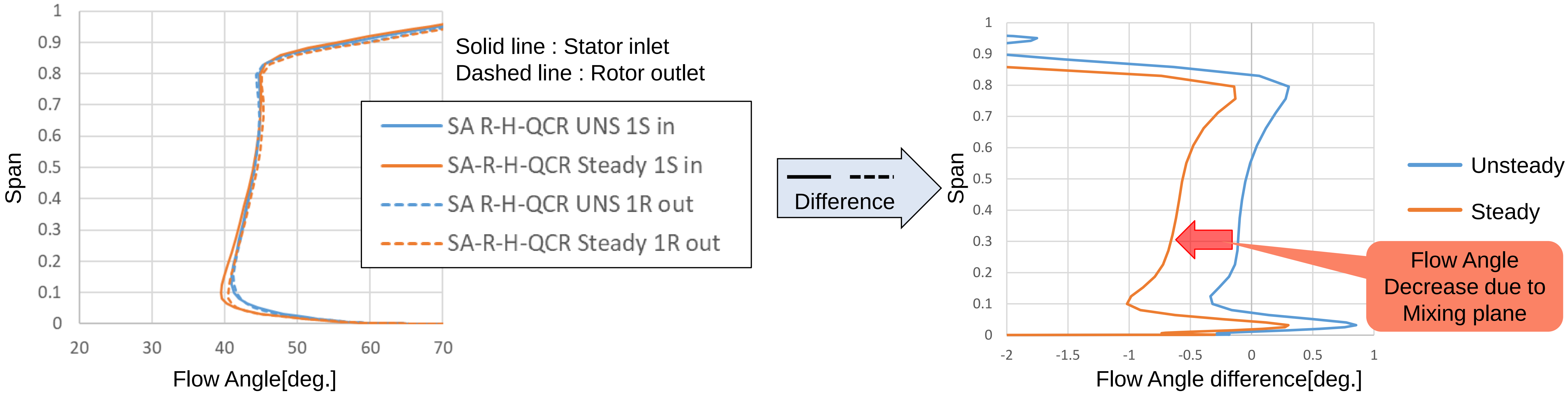

Schematic image of a difference between steady and unsteady case

Steady CFD

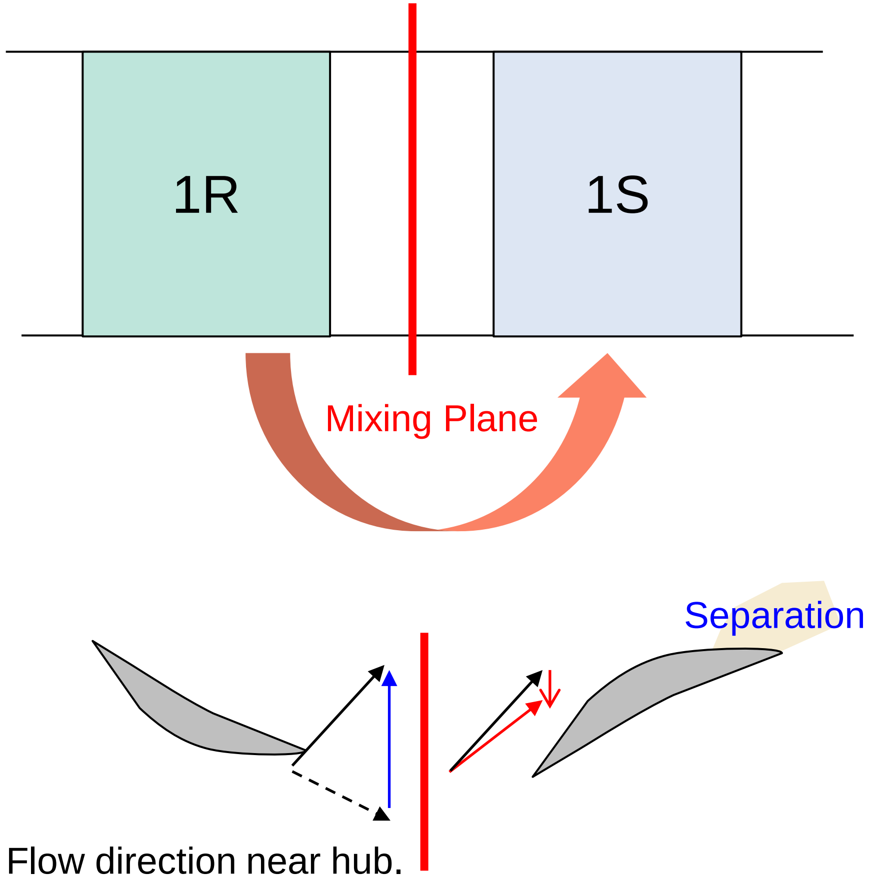

- Angle of attack for stator becomes small.

Unsteady CFD

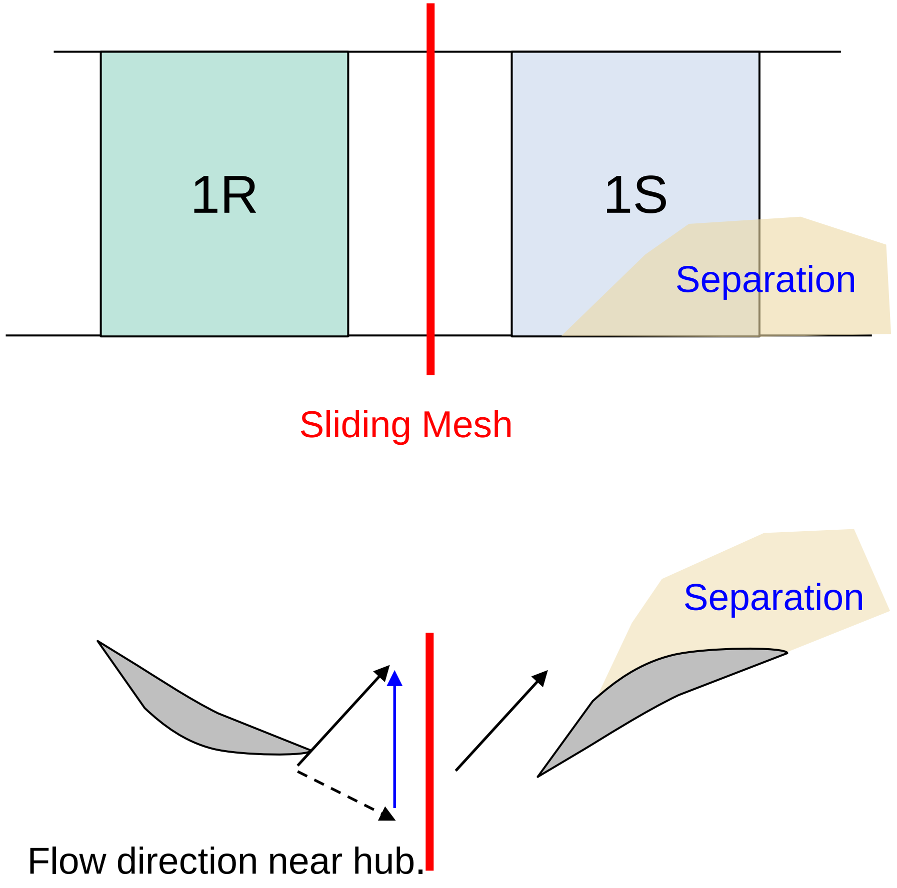

- Relatively high angle of attack in unsteady CFD.
- Massive corner separation is generated.
- Blockage becomes high and small pressure rise is derived.

Summary

Summary

IHI

Steady Analysis: SA vs. SA-R-H-QCR2000

- Static pressure rise coefficient shows slightly higher than that of experiment.
- Optimized R-H-QCR show smaller stall mass flow coefficient than that of pure SA model.
- Internal flow at stator differs from experimental result.

Unsteady CFD with SA-R-H-QCR2000

- Unsteady R-H-QCR model shows better agreement at high flow rate condition, however, stall mass flow coefficient becomes higher in unsteady case.
- Massive hub corner separation is observed in unsteady CFD at stator.
- This difference caused by flow angle difference at mixing plane.

Still remaining questions

- There still exist discrepancy even with URANS on stall massflow.
- Investigation and improvement on flow angle difference by mixing plane should be carried out. Unsteady CFD cannot be applied for design CFD even now.

IHI

Realize your dreams

GPPS Chania22, September 11, 2022
CFD Workshop

Validation of improved SA model on Various Cascades
Part2 : Numerical Simulation Result on TUDA cascade

2022/9/11

IHI Corporation
Core Technology & System Engineering Gr.
Advanced Technology Department
Research & Engineering Division
Naoki Tani

IHI

For CFD workshop

- Validation and verification of RANS analysis

  Comparison of other CFD code at the same RANS model can reveal each solver characteristics.

For CFD technology development

- Validation of improved RANS
  - ➢ There are several researches on improved RANS model, however, validation cases with these improved models are limited.
    - ➢ This CFD workshop is good chance to validate improved model.
  - ➢ Impact of unsteady CFD was also validated.

TUD cascade is appropriate for High Mach number validation.

CFD code : UPACS

- UPACS (Originally developed by JAXA)
- Cell centered
- Multi block structured grid

Kazawa, Junichi, et al. "Numerical study on fan noise generated by rotor-stator interaction." 13th AIAA/CEAS Aeroacoustics Conference (28th AIAA Aeroacoustics Conference). 2007.

- MUSCL interpolated 3rd order scheme
- Matrix free Gauss-Sidel time integration
  - 2nd order accuracy in time with newton sub-iteration
- Buffer-layer type non-reflective mixing plane
- Spallart-Allmaras turbulence model
  - SA and optimized SA-R-H-QCR2000(Steady and Unsteady)
- Density base solver
  - No low Mach-number preconditioning

Blue character part is different from BUAA cases.

IHI

Classical mixing plane

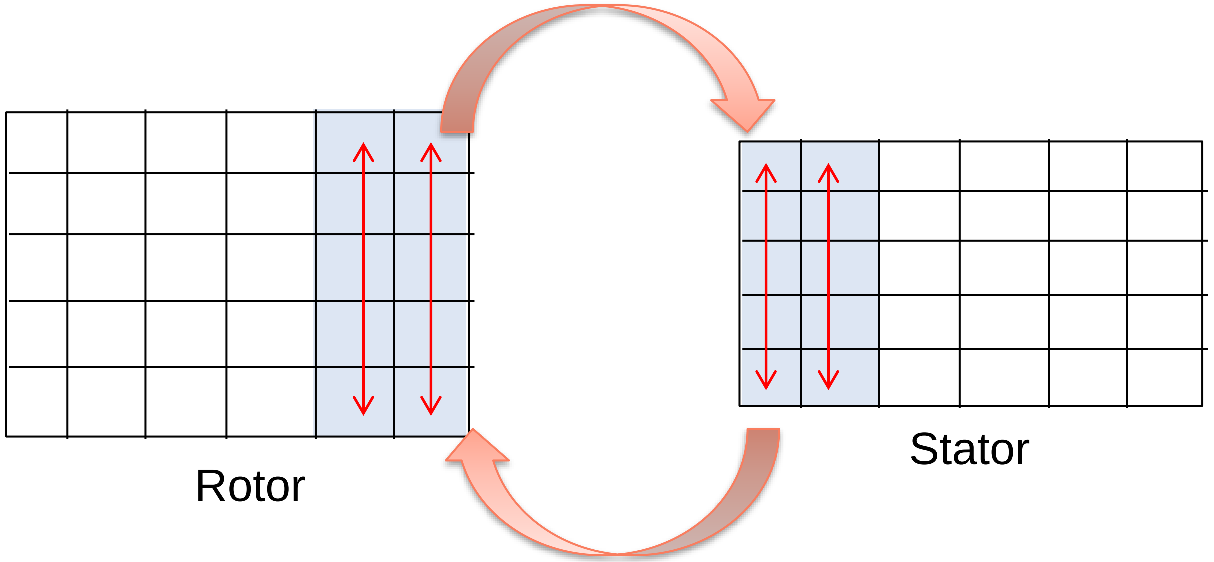

1. Circumferential averaging
2. Exchange data between R/S
3. NRBC operation (option)

Buffer-layer type non-reflective mixing plane

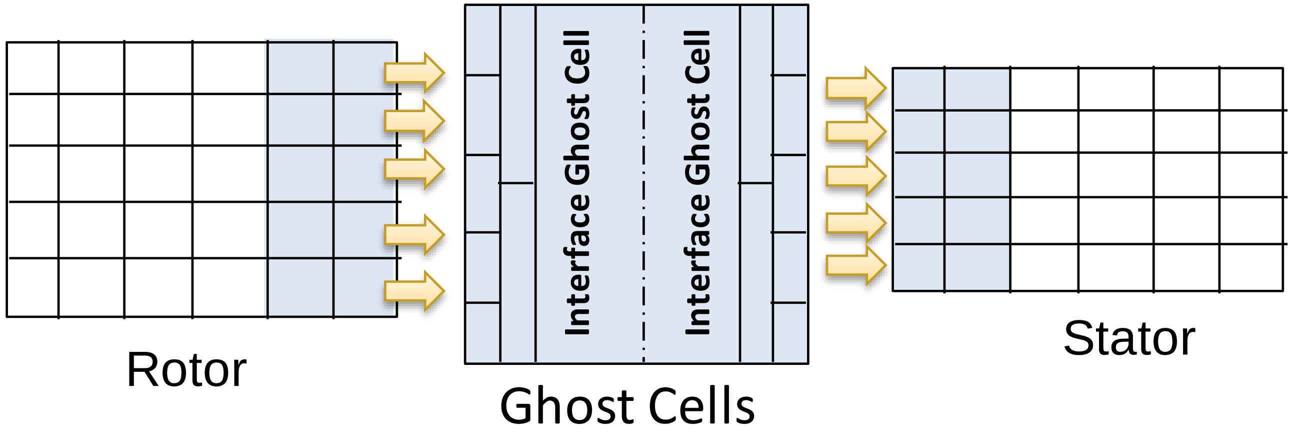

1. Generate ghost cells between R/S.
2. Coarsening to 1 cell at the interface.
3. Both inner and ghost cells are solved simultaneously

Turbulence model: SA-R-H-QCR2000

IHI

Matsui K., et al. “CALIBRATED ROTATION-HELICITY-QUADRATIC CONSTITUTIVE RELATION SPALARTALLMARAS (R-H-QCR SA) MODEL FOR THE PREDICTION OF MULTI-STAGE COMPRESSOR CHARACTERISTICS.” *Proceedings of ASME Turbo Expo 2022Turbomachinery Technical Conference and Exposition, GT2022-82080*

SA-R-H-QCR2000

SA-R: Rotation correction.

Reduce turbulence generation at rigid rotation part.

$$S_{SA-R} = S_{SA} + C_{rot} min(0, S - \Omega)$$

SA-H: Helicity modification.

Consideration of turbulence backscatter.

$$f_h = 1 + c_{h1} \widehat{H}^{c_{h2}}$$

$$\widehat{H} = \frac{\boldsymbol{u} \cdot \boldsymbol{\Omega}}{|u||\Omega|}$$

SA-QCR2000: Quadratic Constitutive Relation.

SA model which can consider anisotropic effect.

$$\tau_{ij_{QCR}} = \tau_{ij} - C_{cr1}\left[O_{ik}\tau_{jk} + O_{jk}\tau_{ik}\right], \qquad C_{cr1} = 0.3$$

$$O_{ij} = 2W_{ij} \Big/ \sqrt{\frac{\partial u_m}{\partial x_n}\frac{\partial u_m}{\partial x_n}}, W_{ij} = \frac{1}{2}\left(\frac{\partial u_i}{\partial x_j} - \frac{\partial u_j}{\partial x_i}\right)$$

Mode constants are optimized with Polynomial Chaos Method.

Computational grid and boundary conditions

IHI

Official grid was not used.

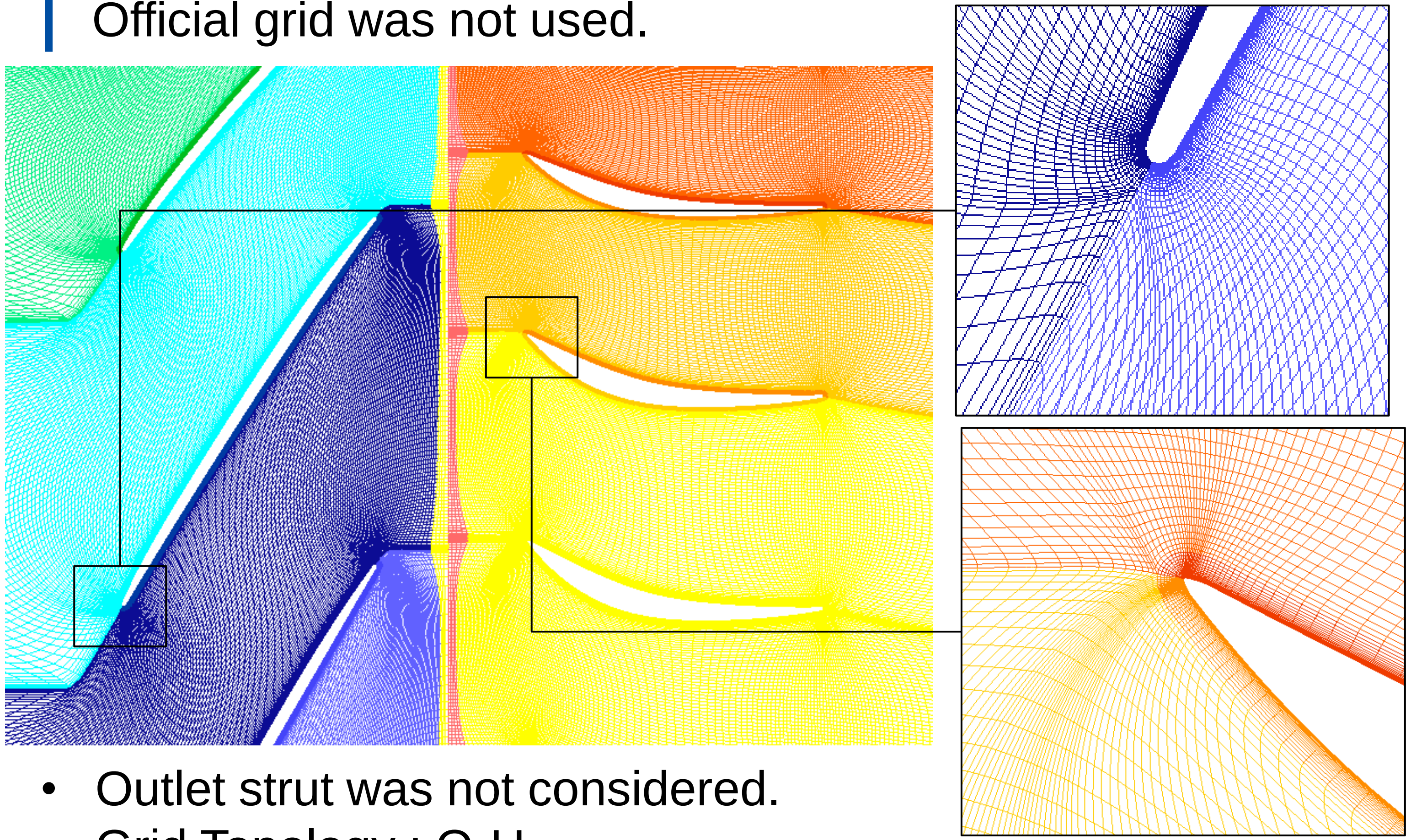

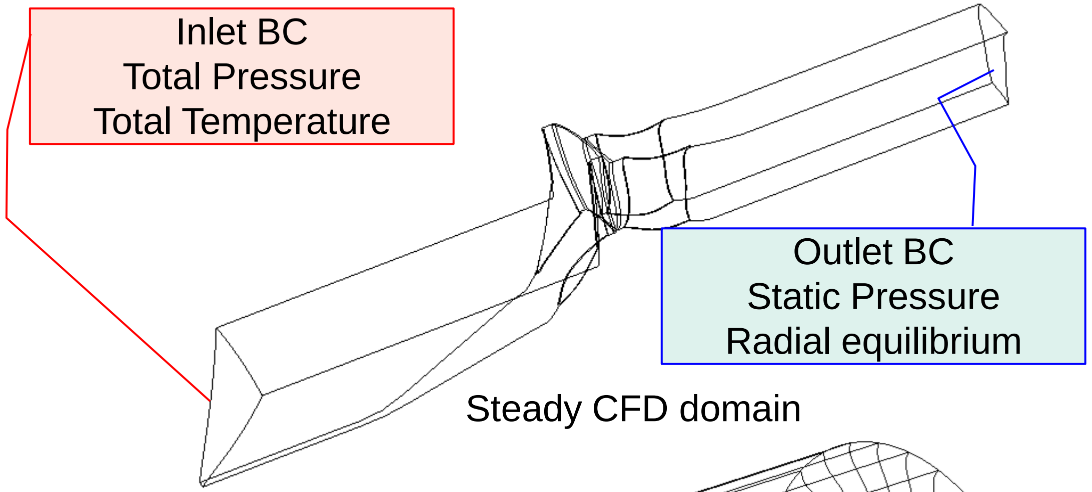

Steady CFD domain

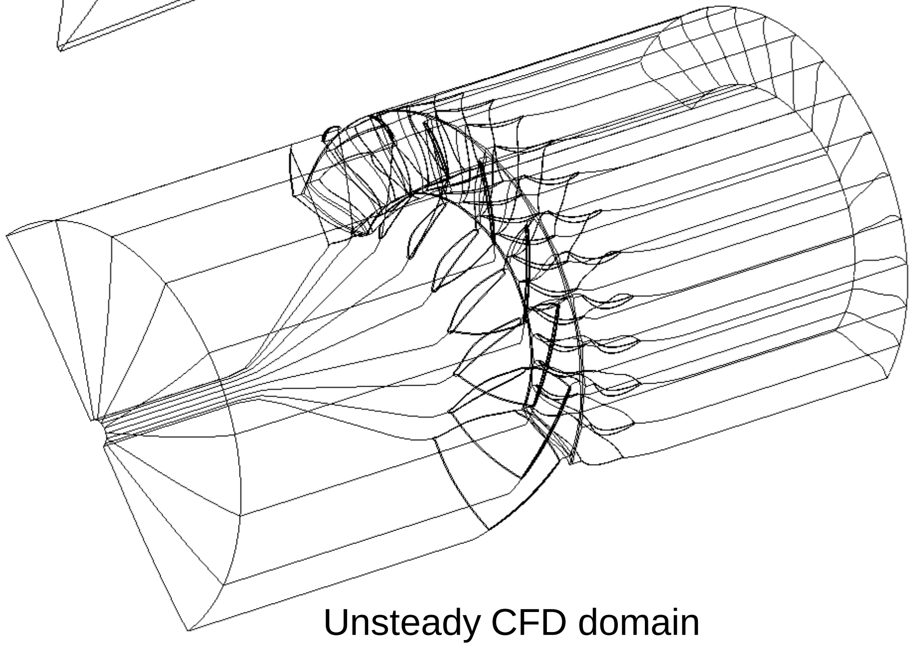

Unsteady CFD domain

- Outlet strut was not considered.
- Grid Topology : O-H
  - Max centroid skewness is 0.95
  - Y+~3 with 1.2 growth rate
- Total grid point : 3.4M(Steady) and 38M(Unsteady 1/2 round)
- Computational resources
  - Steady : 20 cores 12 hours per case
  - Unsteady : 40 cores 20 hours 4 rotation per case

	Blade Count	Scaled Blade Count for Unsteady CFD
1R	16	16
1S	29	30

Computational results

Overall performance comparison

IHI

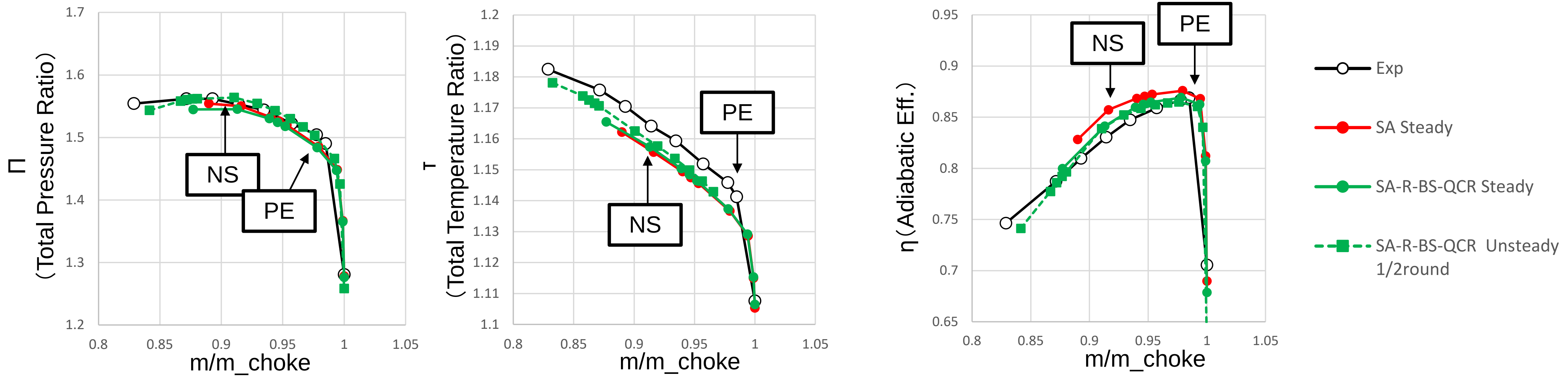

UPACS CFD results

- Stall flowrate of modified SA (SA-R-H-QCR) show slightly smaller than that of SA.
- Unsteady CFD can calculate smaller flowrate than steady CFD.

- Total temperature ratio is relatively smaller than experimental data, therefore, efficiency becomes slightly higher.

- Question : Why unsteady CFD can get result at “positive slope” Π-m region?

- Experimental total pressure shows smaller near shroud.
  - All CFD results show relatively flat distribution.
  - It should be noted overshoot near shroud cannot be seen at ★ point.
- Flow angle show reasonably fine result in all CFD result.

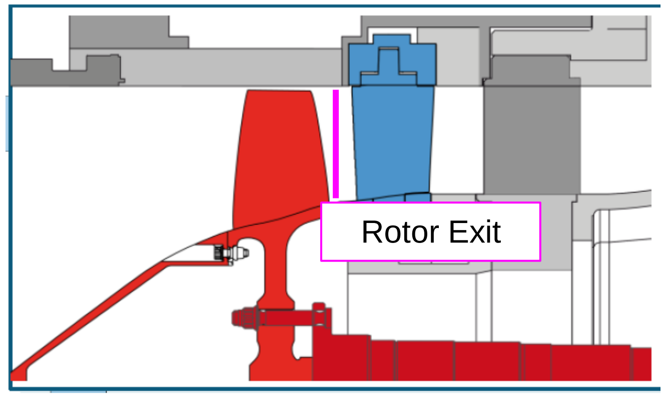

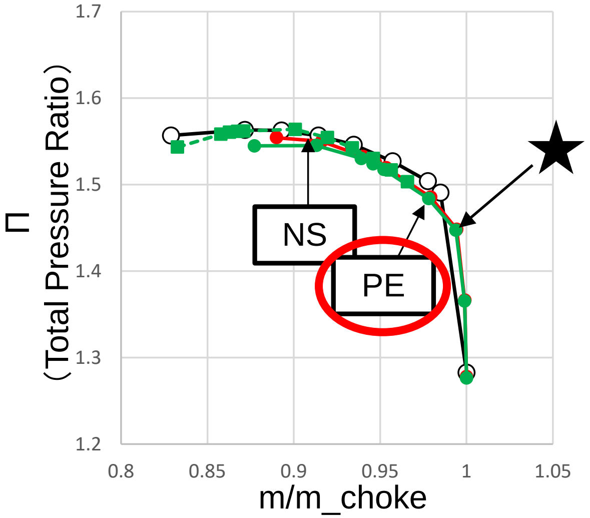

Total pressure distribution at ★ point.

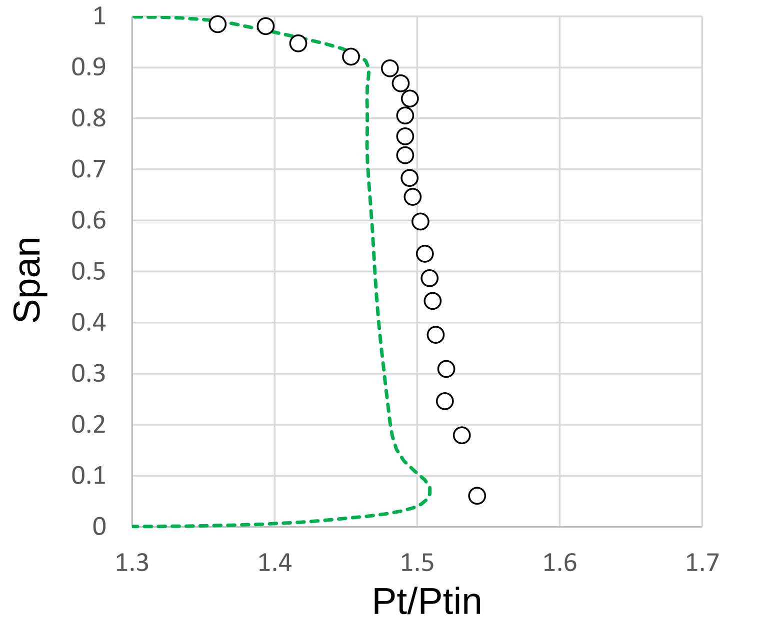

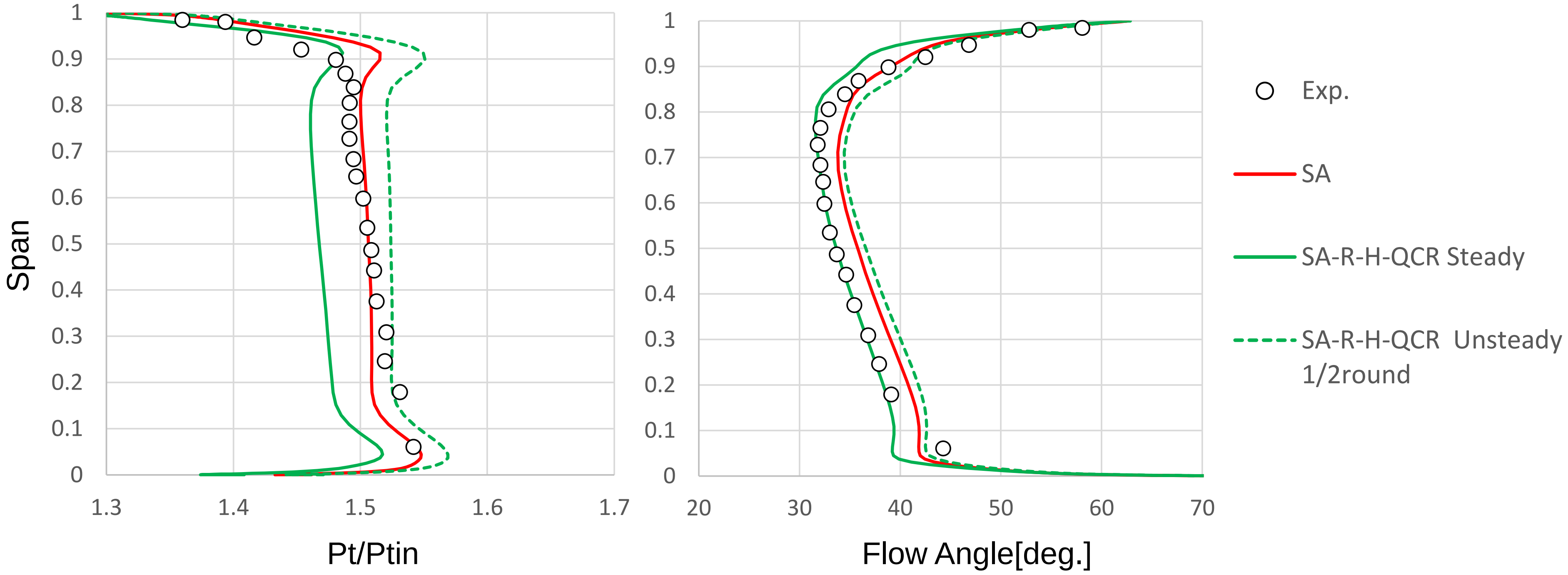

Stator exit distribution at PE condition : Spanwise distribution

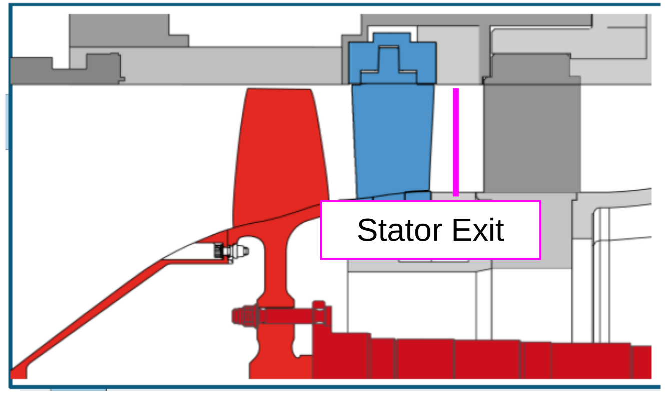

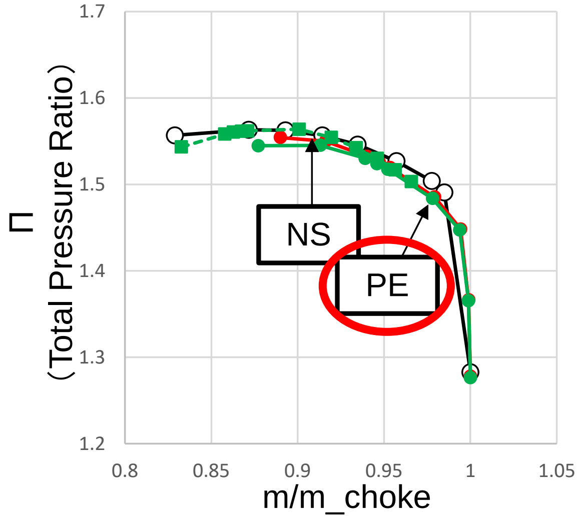

- Pt distribution of CFD show relatively flat distribution. This tendency is the same as rotor exit.
- Total temperature distribution agrees well especially with SA-R-H-QCR unsteady case.

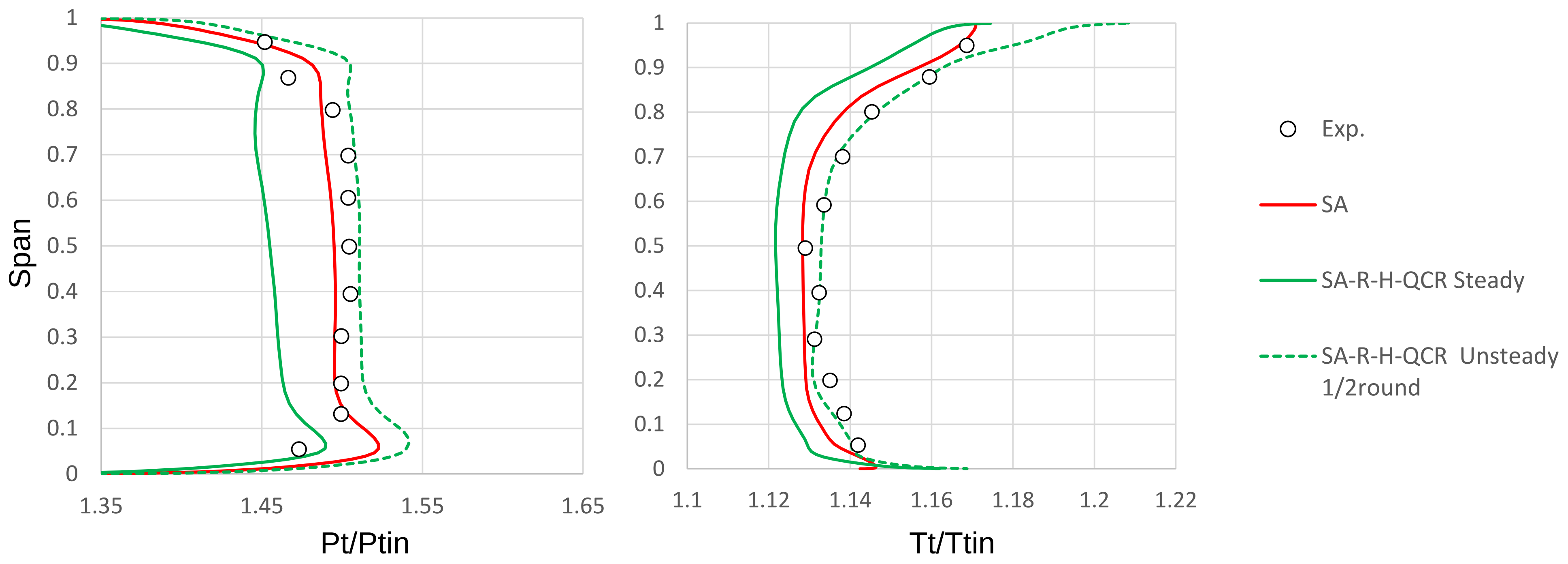

Stator exit distribution at PE condition : 2D distribution

IHI

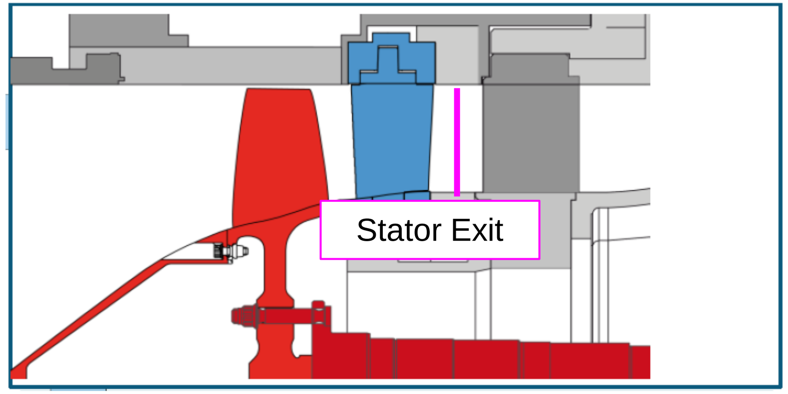

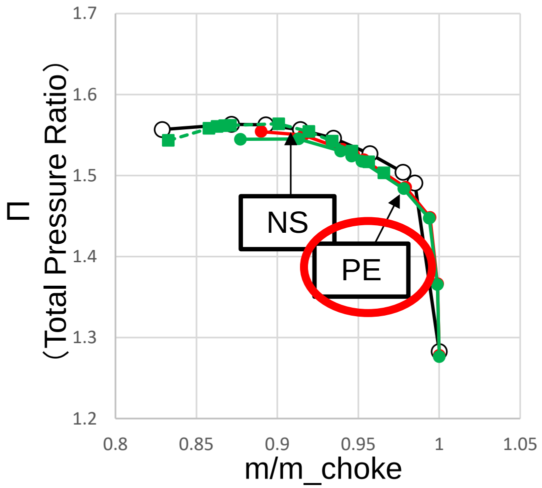

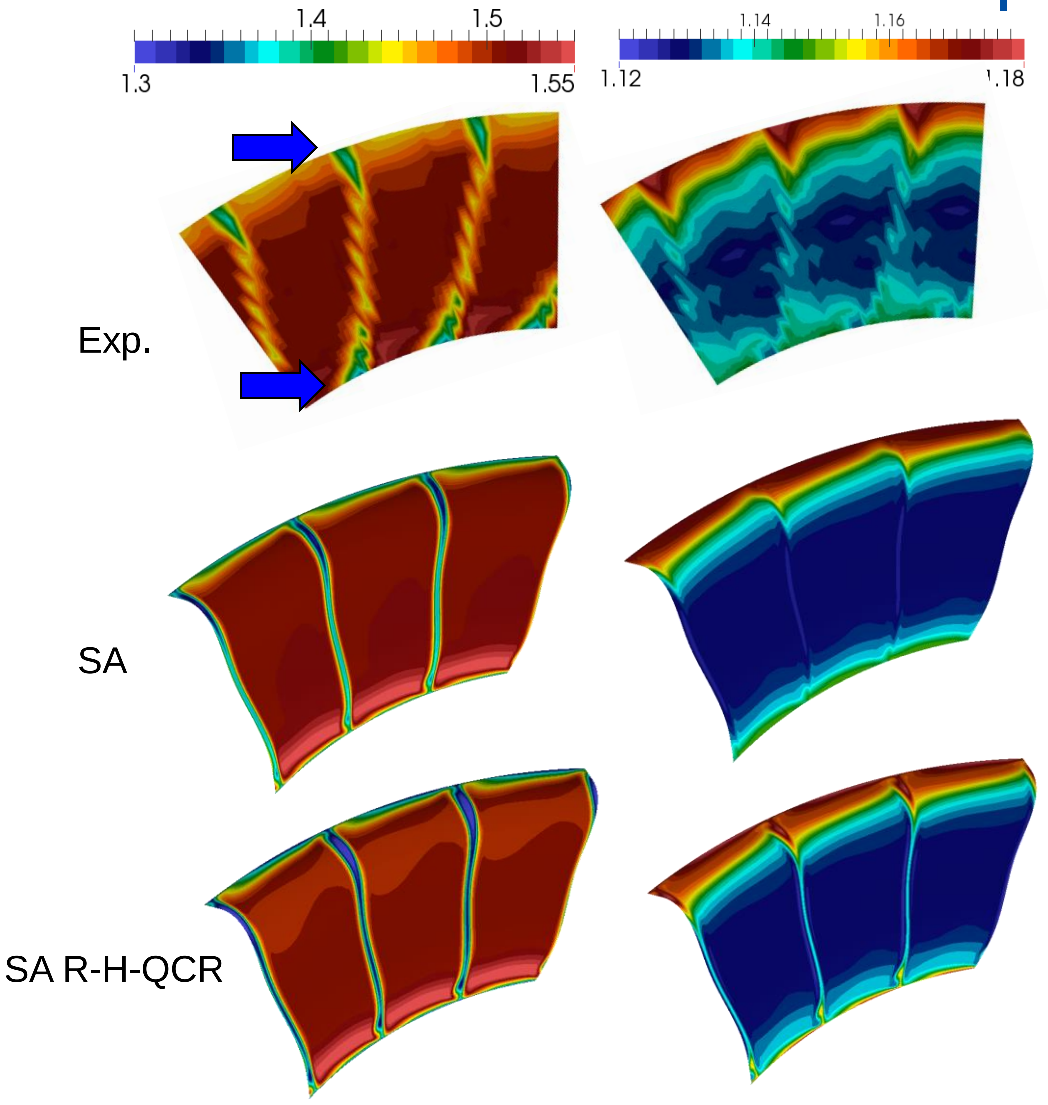

Total Pressure (Pt/Ptin)

Total Temperature (Tt/Ttin)

Low pressure region near hub and tip (blue allow) cannot be seen in CFD. This causes overprediction near hub and tip.

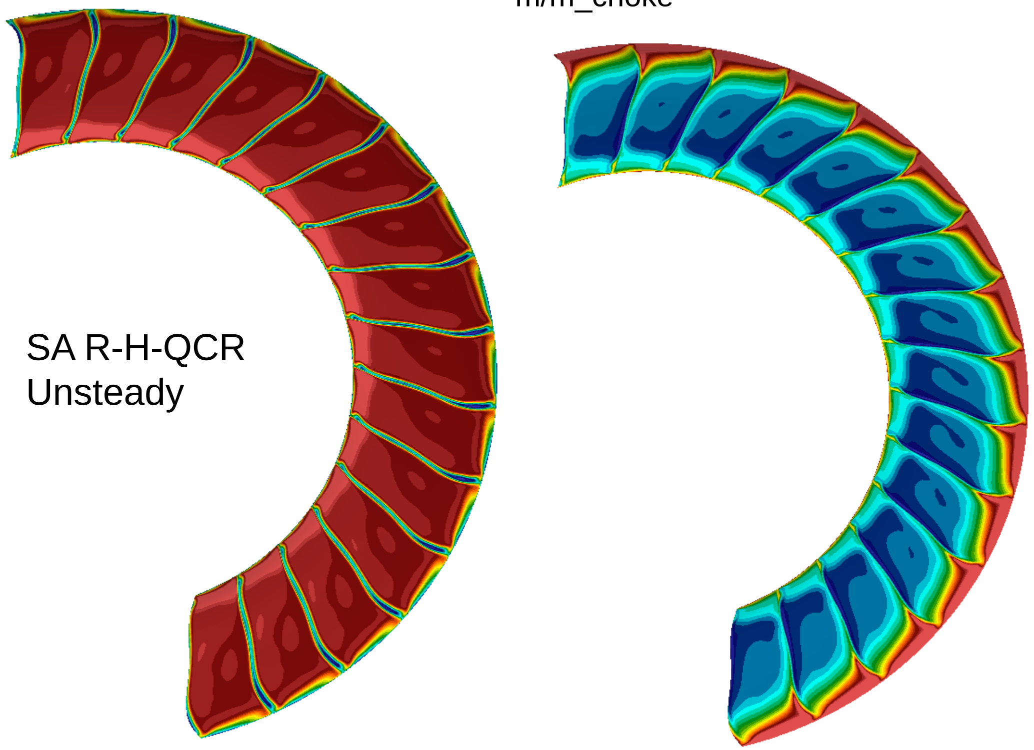

Total Pressure (Pt/Ptin)

Total Temperature (Tt/Ttin)

Stator exit distribution at NS condition : Spanwise distribution

IHI

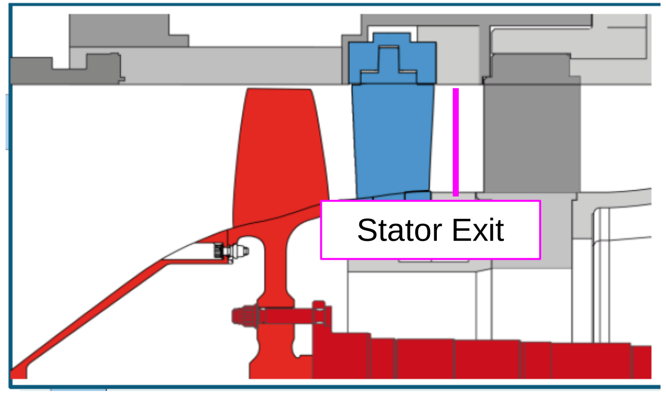

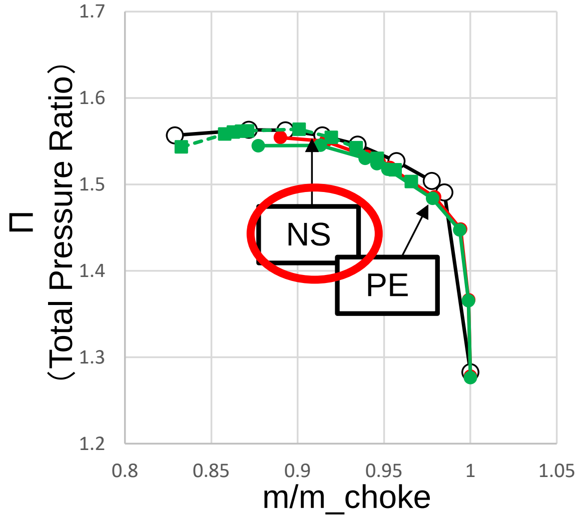

- Total pressure distribution near shroud show good agreement, however, overshoot can be observed near hub.
- Total pressure distribution is reasonable for all CFD cases.

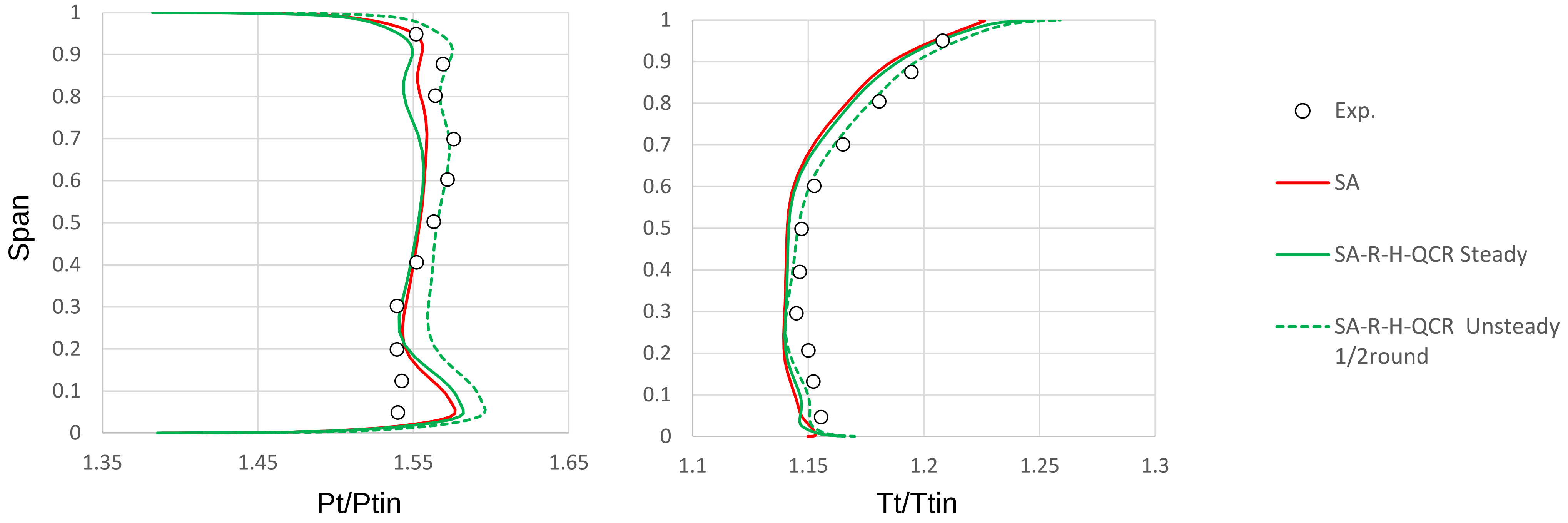

Stator exit distribution at NS condition : 2D distribution

IHI

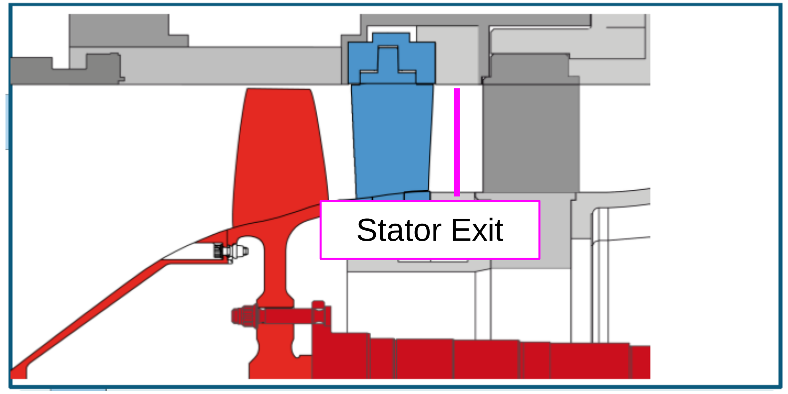

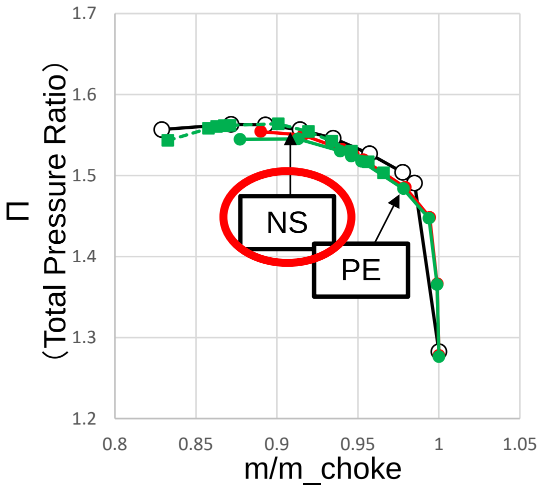

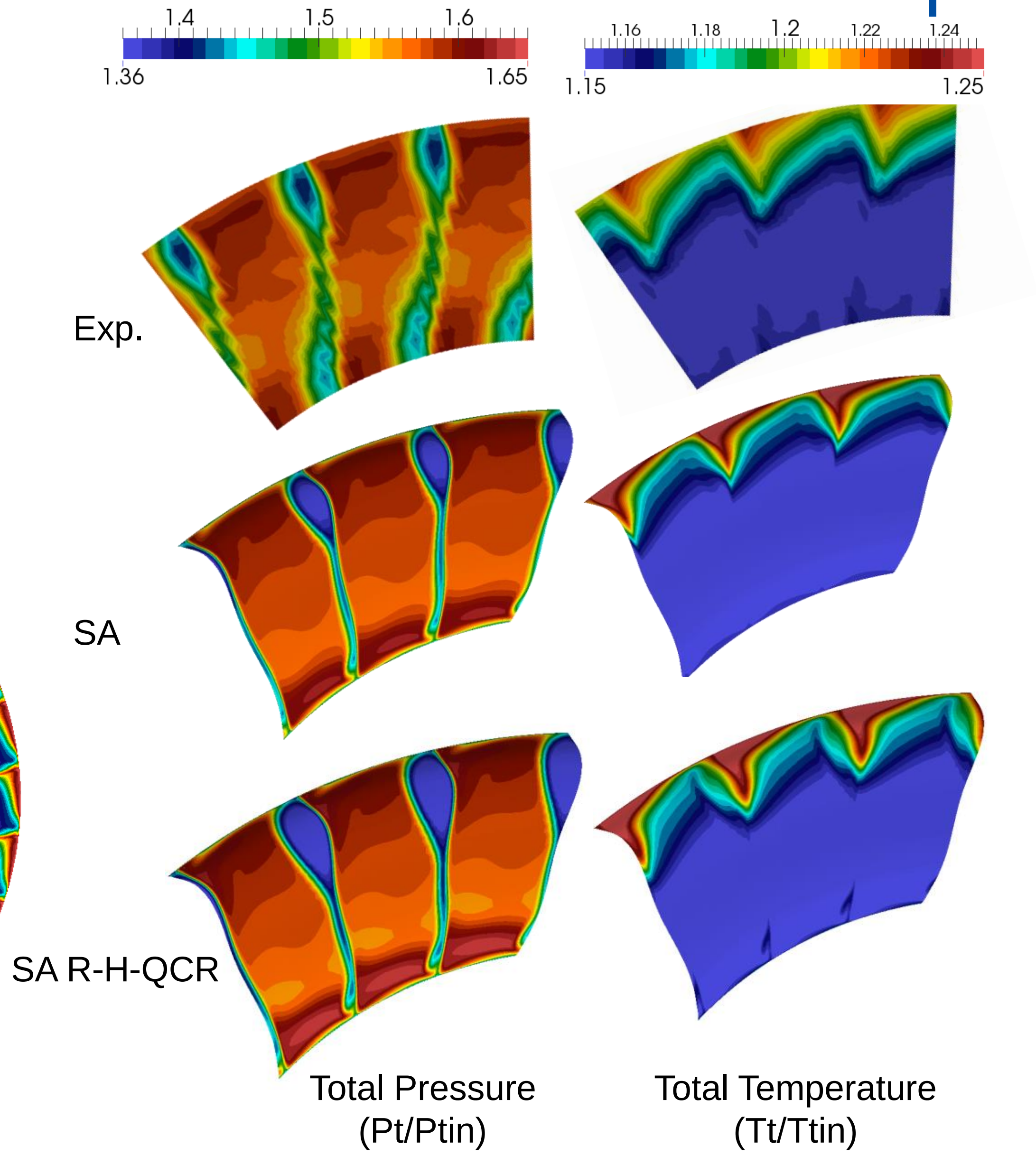

Total pressure drop due to separation can be observed near shroud.

- Unsteady case show smaller separation region.
- Snapshot shows circumferential total pressure disturbance.

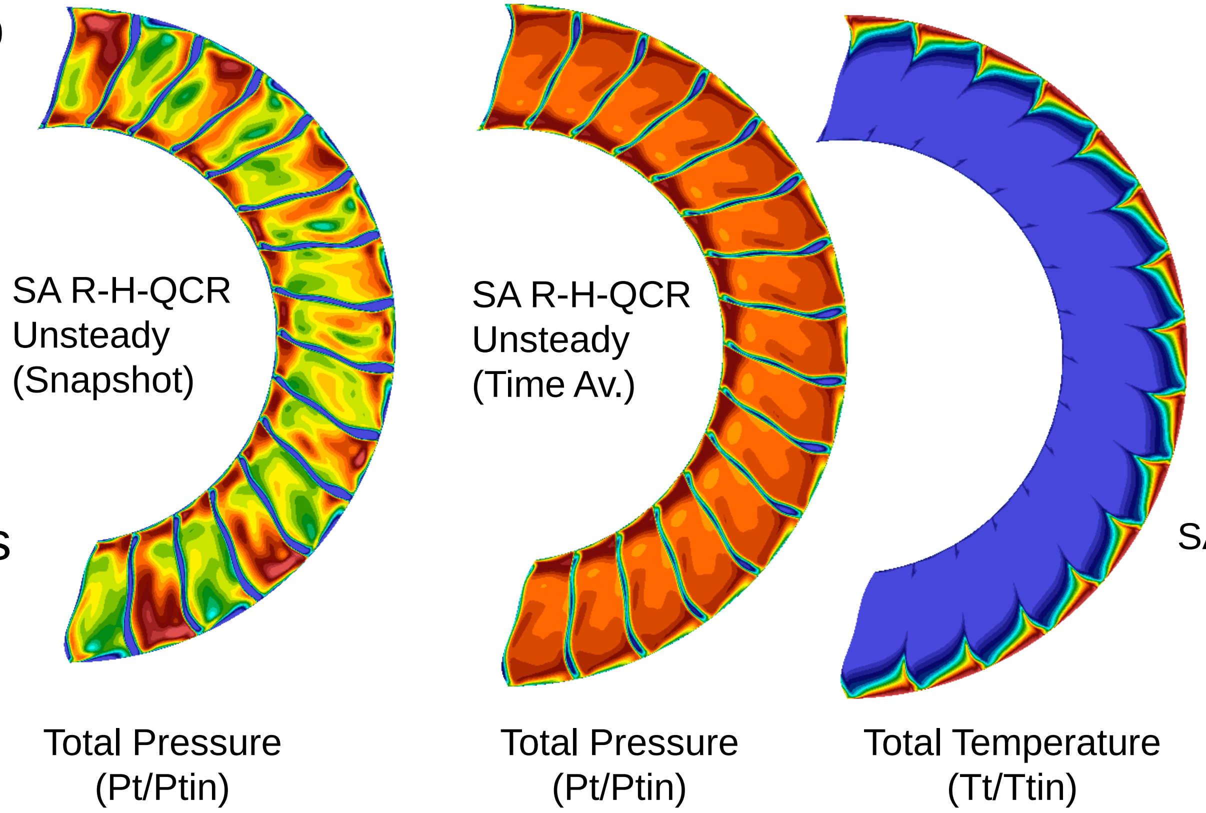

Unsteady CFD result at positive slope

IHI

Unsteady CFD could calculate positive slope region.

Static pressure was applied at outlet boundary.

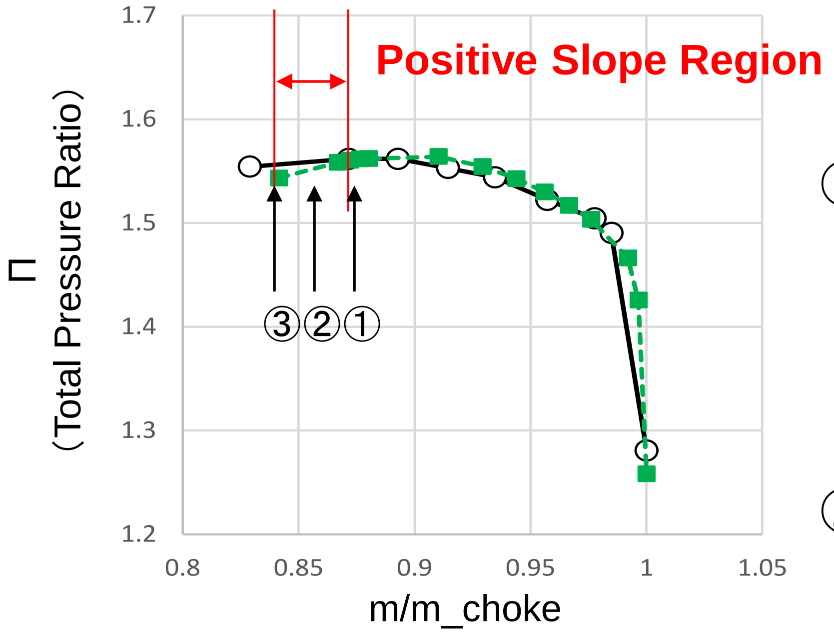

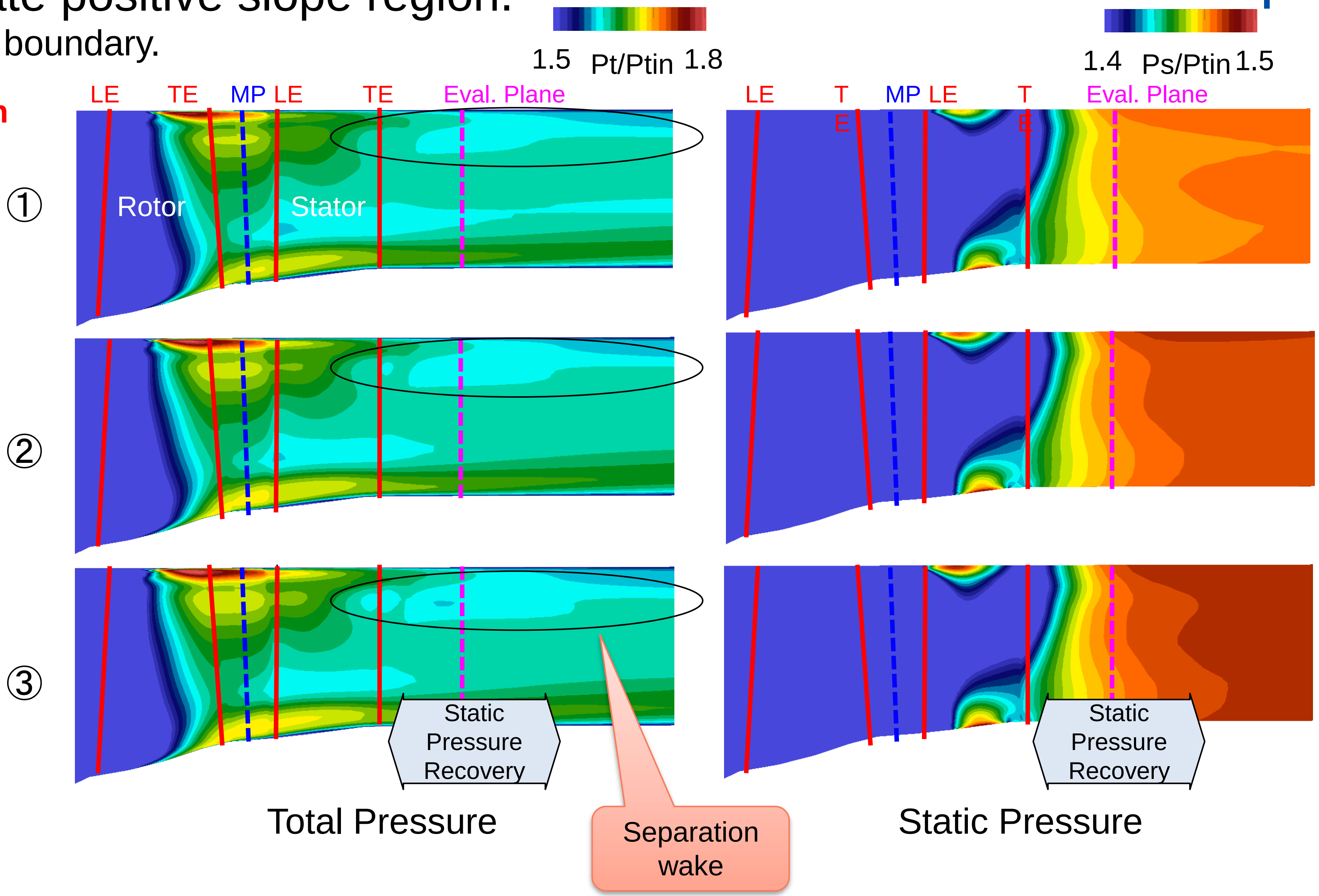

- Separation region works as “diffuser passage”.
- Static pressure recovery occurs near stator trailing edge as mass flow is reduced (①to③).

Summary

Summary

IHI

SA, SA-R-H-QCR2000 and Unsteady SA-R-H-QCR2000 were compered.

- Stall flowrate of modified SA (SA-R-H-QCR) show slightly smaller than that of SA.
- Unsteady CFD can calculate smaller flowrate than steady CFD.
  - This is caused by diffuser passage generation at stator exit.
- Spanwise distribution also shows good agreement with unsteady CFD except for total pressure overshoot near hub.

Still remaining questions

- Unsteady CFD result was fine, however, it has not yet been validated whether unsteady phenomena can be reproduced or not.
- Presently, outlet strut was not considered. Impact of outlet strut must be carried out.

IHI

Realize your dreams